Case Studies in Thermal Engineering 4 (2014) 15–23

Contents lists available at ScienceDirect

Case Studies in Thermal Engineering

journal homepage: www.elsevier.com/locate/csite

Scrutiny of mixed convection flow of a nanofluid in a vertical channel

M. Fakour [a,*], A. Vahabzadeh [a], D.D. Ganji [b]

[a] Department of Mechanical Engineering, Sari Branch, Islamic Azad University, Sari, Iran
[b] Department of Mechanical Engineering, Babol University of Science and Technology, Babol, Iran

ARTICLE INFO

Article history:
Received 24 April 2014
Received in revised form
15 May 2014
Accepted 16 May 2014
Available online 23 May 2014

Keywords:
Nanofluid
Vertical channel
Mixed convection
Homotopy perturbation method (HPM)

ABSTRACT

The laminar fully developed nanofluid flow and heat transfer in a vertical channel are investigated. By means of a new set of similarity variables, the governing equations are reduced to a set of three coupled equations with an unknown constant, which are solved along with the corresponding boundary conditions and the mass flux conservation relation by the homotopy perturbation method (HPM). We have tried to show reliability and performance of the present method compared with the numerical method (Runge–Kutta fourth-rate) to solve this problem. The effects of the Grashof number (Gr), Prandtl number (Pr) and Reynolds number (Re) on the nanofluid flows are then investigated successively. The effects of the Brownian motion parameter (N_b), the thermophoresis parameter (N_t), and the Lewis number (L_e) on the temperature and nanoparticle concentration distributions are discussed. The current analysis shows that the nanoparticles can improve the heat transfer characteristics significantly for this flow problem.
© 2014 The Authors. Published by Elsevier Ltd. This is an open access article under the CC BY license (http://creativecommons.org/licenses/by/3.0/).

1. Introduction

Mixed convection flows or combined free and forced convection flows occur in many technological and industrial applications in nature, e.g., solar receivers exposed to wind currents, electronic devices cooled by fans, nuclear reactors cooled during emergency shutdown, heat exchangers placed in a low-velocity environment, flows in the ocean and in the atmosphere and so on. The comprehensive reviews of convective flows are given in the monograph by Gebhart et al. [1] and Martynenko and Khramtsov [2]. A technique for improving heat transfer uses solid particles in the base fluids, which has been used recently in some studies. The term nanofluid refers to fluids in which nano-scale particles are suspended in the base fluid, which was initially suggested by Choi [3]. The comprehensive references on nanofluids have been done by Yu and Lin [4], Das et al. [5], Buongiorno [6], Daungthongsuk and Wongwises [7], Ding et al. [8], Wang and Mujumdar [9,10], and Kaka and Pramuanjaroenkij [11]. In most heat transfer studies, the base fluid has a low thermal conductivity, which limits the heat transfer enhancement. However, the continuing miniaturization of electronic devices requires further heat transfer improvements from an energy saving viewpoint. An innovative technique for adding nanoparticles to the base fluid was introduced by Choi [3] for heat transfer enhancement of pure fluids. The resulting mixture of the base fluid and nanoparticles has unique physical and chemical properties. It is expected that the presence of nanoparticles in the

* Corresponding author. Tel.: +989119579177.
E-mail addresses: mehdi_fakour@yahoo.com, mehdi_fakoor8@yahoo.com (M. Fakour), Vahabzadeh_a@yahoo.com (A. Vahabzadeh), ddg_davood@yahoo.com (D.D. Ganji).

http://dx.doi.org/10.1016/j.csite.2014.05.003
2214-157X/© 2014 The Authors. Published by Elsevier Ltd. This is an open access article under the CC BY license (http://creativecommons.org/licenses/by/3.0/).

Table 1
The result of HPM and numeric method for U, θ and φ.

y	HPM(U)	NUM(U)	HPM(θ)	NUM(θ)	HPM(φ)	NUM(φ)
−1.0	0.00000007	0.0000000000	0.0000000078	1.0000000000	−0.0000000069	0.0000000000
−0.8	0.0015258029	0.0015322789	0.0353431520	0.0353488532	−0.0415288519	−0.0414708272
−0.6	0.028889823	0.0029013226	0.0627668542	0.0627767997	−0.0745248639	−0.0744174086
−0.4	0.0039582922	0.0039752697	0.0823183873	0.0823313032	−0.0984913012	−0.0983461175
−0.2	0.0046384449	0.0046583907	0.0940340772	0.0940487521	−0.1130375452	−0.1128687272
0.0	0.0048716232	0.0048925940	0.0979367194	0.0979519717	−0.1179147516	−0.1177378758
0.2	0.0046384449	0.0046583907	0.0940340772	0.0940487521	−0.1130375452	−0.1128687272
0.4	0.0039582922	0.0039752697	0.0823183873	0.0823313032	−0.0984913012	−0.0983461175
0.6	0.0028889823	0.0029013226	0.0627668542	0.0627767997	−0.0745248639	−0.0744174086
0.8	0.0015258029	0.0015322789	0.0353431520	0.0353488532	−0.0415288519	−0.0414708272
1.0	0.0000000007	0.0000000000	0.0000000078	0.0000000000	−0.0000000069	0.00000000000

nanofluid increases the thermal conductivity and therefore substantially enhances the heat transfer characteristics of the nanofluid. Eastman et al. [12] and Xie et al. [13] showed that higher thermal conductivity can be achieved in thermal systems using nanofluids. Moreover, it is well-known that conventional heat transfer fluids, including oil, water, and ethylene glycol mixture, are poor heat transfer fluids, since the thermal conductivity of these fluids plays an important role on the heat transfer coefficient between the heat transfer medium and the heat transfer surface. Researchers have tried to increase the thermal conductivity of base fluids by suspending micro- or larger-sized solid particles in fluids, since the thermal conductivity of solid is typically higher than that of liquids, as seen from Table 1 in the paper by Oztop and Abu-Nada [14]. Nanofluids consist of very small-sized solid particles. Therefore, in a low solid concentration, it is reasonable to consider the nanofluid as a single phase flow (Xuan and Li [15]). There are many numerical studies about heat and mass transfer of nanofluids in enclosures. In contrary, the number of studies on natural and mixed convection of nanofluids in vertical and horizontal channels is very small [16]. However, several researches on nanofluid flows in pipes and bends have been available in the literature, as shown by Lin et al. [17] and Lin and Lin [18]. We mention to this end the very interesting paper by Lavine [19] on steady fully developed opposing mixed convection between inclined parallel plates filled by a viscous and incompressible fluid (a regular fluid). The present paper considers the steady fully developed mixed convection flow in a vertical channel filled with nanofluids, which is driven by an external pressure gradient and also by a buoyancy force using the mathematical nanofluid model proposed by Buongiorno [6]. The paper may be regarded as the extension of the problem considered by Chen and Chung [20] on the mixed convection of a viscous (Newtonian) fluid in a vertical channel with linear variation of the wall temperature. Using similarity variables, the governing partial differential equations are transformed to ordinary differential equations, which are solved along with the corresponding boundary conditions and the mass flux conservation relation by the homotopy perturbation method (HPM) [22–25]. To our best knowledge, this problem has not been considered before so that the results are new and original.

2. Describe problem and mathematical formulation

In the present study the laminar fully developed nanofluid flow and heat transfer in a vertical channel are investigated which is driven by an external pressure gradient and also by a buoyancy force. Fig. 1 shows the physical model. As can be seen in this figure the origin of coordinates is considered at the center of the channel. The gravitational acceleration vector g is perpendicular to the y-axis. The parameters u and v are the velocity components in x and y directions, respectively. The temperature distribution at the both of the walls and the nanoparticle volume fraction on the walls are defined as follows: $T_w(x)=T_0+A_1x$, $C_w(x)=C_0+A_2x$; where T_0 is a reference temperature at the channel entrance and A_1 is a constant and C_0 denotes the nanoparticle volume fraction at far field and A_2 is a positive constant. Equations of the conservation of total mass, momentum, thermal energy, and nanoparticle volume fraction with considering the nanofluid model proposed by Buongiorno [6] and introducing the Oberbeck–Boussinesq approximation by Kuznetsov and Nield [21] can be presented

$$\frac{\partial u}{\partial x}+\frac{\partial v}{\partial y}=0, \tag{1}$$

$$\frac{\partial p}{\partial x}=\mu\frac{\partial^2 u}{\partial y^2}+\left[(1-C_0\,\rho_f\,\beta(T-T_w)-(\rho_s-\rho_f)(C-C_w)\right]g, \tag{2}$$

$$\alpha\frac{\partial^2 T}{\partial y^2}+\tau\left\{D_B\left(\frac{\partial C}{\partial x}\frac{\partial T}{\partial x}+\frac{\partial C}{\partial y}\frac{\partial T}{\partial y}\right)+\left(\frac{D_T}{T_0}\right)\left[\left(\frac{\partial T}{\partial x}\right)^2+\left(\frac{\partial T}{\partial y}\right)^2\right]\right\}=u\frac{\partial T}{\partial x}, \tag{3}$$

$$D_B\frac{\partial^2 C}{\partial y^2}+\left(\frac{D_T}{T_0}\right)\left(\frac{\partial T}{\partial y}\right)^2=u\frac{\partial C}{\partial x}, \tag{4}$$

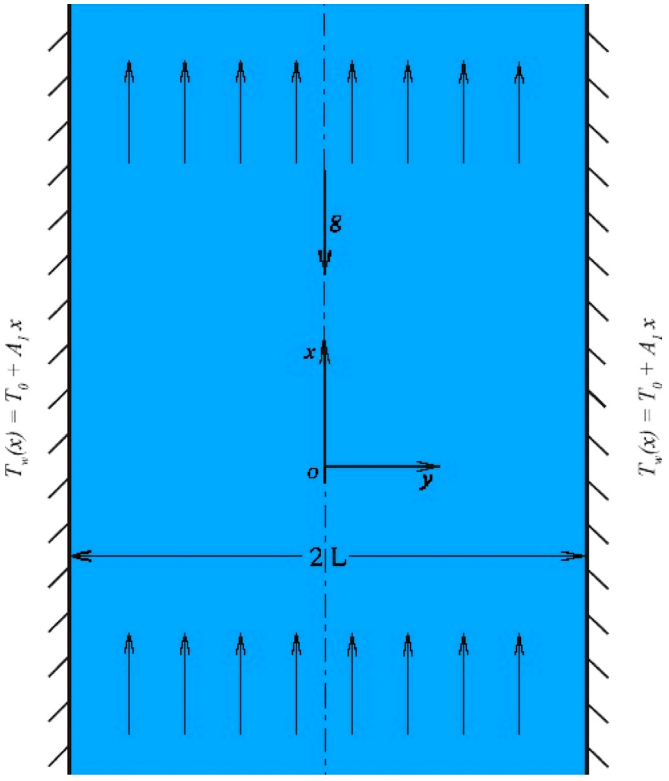

Fig. 1. Schematic of the geometry and coordinate system.

subject to the boundary conditions

$$u(-L)=0, \quad u(+L)=0, \quad T_w(x)=T_0+A_1x, \quad C_w(x)=C_0+A_2x, \tag{5}$$

where μ, β and α are, respectively, the dynamic viscosity, the volumetric expansion coefficient and the thermal diffusivity of the nanofluid, ρ_f is the base fluid density and ρ_s is the nanoparticle mass density, and τ is a parameter defined by $\tau=(\rho c)_s/(\rho c)_f$ with $(\rho c)_s$ being heat capacity of the nanoparticle and $(\rho c)_f$ being the heat capacity of fluid.

It is a common practice in channel flow studies to assume the mass flow rate as a prescribed quantity; where U_m is defined as the average fluid velocity in the channel section

$$U_m=\frac{1}{2L}\int_{-L}^{L}u(y)dy=\frac{1}{L}\int_0^1 u(y)dy. \tag{6}$$

Dimensionless variables are as follows:

$$X=\frac{x}{L}, \quad Y=\frac{y}{L}, \quad U(Y)=\frac{Re\,Pr}{U_m}u, \quad \theta(Y)=\frac{T-T_w}{A_1L},$$
$$\varphi(Y)=\frac{C-C_w}{A_2L}, \quad P(X)=\frac{p}{\rho_f U_m^2}. \tag{7}$$

Substituting dimensionless variables Eq. (7) into Eqs. (1)–(4), can be obtained [26]

$$U''+(Gr\times Pr)\theta-N_r\varphi+\sigma=0, \tag{8}$$

$$\theta''+N_b\theta'\varphi'+N_t(\theta')^2+N_b+N_t-U=0, \tag{9}$$

$$\varphi''+\frac{N_t}{N_b}\theta''-L_eU=0, \tag{10}$$

Considering the boundary conditions

$$U(1)=U(-1)=0, \quad \theta(1)=\theta(-1)=0, \quad \varphi(1)=\varphi(-1)=0, \tag{11}$$

along with the mass flux conservation relation

$$\int_0^1 U dy = RePr, \tag{12}$$

where Gr, Nr, σ, N_b, N_t, L_e and Pr, respectively, are the Grashof number, the buoyancy ratio, the pressure parameter, the Brownian motion parameter, the thermophoresis parameter, the Lewis number, and the Prandtl number witch describe as follows:

$$Gr = \frac{(1-C_0)\beta g A_1 L^4}{\nu^2}, \quad N_r = \frac{(\rho_c - \rho_f)A_2 g L^4}{\alpha\mu}, \quad \sigma = -\frac{\rho_c}{\rho_f} Pr\, Re^2 \frac{dP}{dX},$$
$$N_b = \frac{(\rho c)_s}{(\rho c)_f} D_B \frac{A_2 L}{\alpha}, \quad N_t = \frac{(\rho c)_s}{(\rho c)_f} \frac{D_r}{T_0} \frac{A_1 L}{\alpha}, \quad L_e = \frac{\alpha}{D_B}, \quad Pr = \frac{\nu}{\alpha}. \tag{13}$$

3. Describe homotopy perturbation method and applied to the problem

3.1. Describe homotopy perturbation method

Consider the following function

$$A(u) - f(r) = 0 \tag{14}$$

with the boundary condition of

$$B\left(u, \frac{\partial u}{\partial n}\right) = 0 \tag{15}$$

where $A(u)$ is defined as follows:

$$A(u) = L(u) + N(u) \tag{16}$$

Homotopy-perturbation structure is shown as

$$H(\nu, p) = L(\nu) - L(u_0) + p\, L(u_0) + p\left[N(\nu) - f(r)\right] = 0 \tag{17}$$

or

$$H(\nu, p) = (1-p)[L(\nu) - L(u_0)] + p[A(\nu) - f(r)] = 0 \tag{18}$$

where

$$\nu(r, p): \Omega \times [0, 1] \to R \tag{19}$$

Obviously, considering Eqs. (17) and (18), we have

$$H(\nu, 0) = L(\nu) - L(u_0) = 0, \quad H(\nu, 1) = A(\nu) - f(r) = 0 \tag{20}$$

where $p \in [0,1]$ is an embedding parameter and u_0 is the first approximation that satisfies the boundary condition. The process of the changes in p from zero to unity is that of $\nu(r, p)$ changing from u_0 to ur We consider ν as

$$\nu = \nu_0 + p \times \nu_1 + p^2 \times \nu_2 + \cdots \tag{21}$$

and the best approximation is

$$u = \lim_{p \to 1} \nu = \nu_0 + \nu_1 + \nu_2 + \cdots \tag{22}$$

The above convergence is discussed in [22,25].

3.2. The HPM applied to the problem

A homotopy perturbation method can be constructed as follows:

$$H(U, p) = (1-p)(U'') + p(U'' + (Gr \times Pr)\theta - N_r\varphi + \sigma), \tag{23}$$

$$H(\theta, p) = (1-p)(\theta'') + p(\theta'' + N_b\theta'\varphi' + N_t(\theta')^2 + N_b + N_t - U), \tag{24}$$

$$H(\varphi,p)=(1-p)(\varphi'')+p\left(\varphi''+\frac{N_t}{N_b}\theta''-L_eU\right), \tag{25}$$

One can now try to obtain a solution of Eqs. (23)–(25) in the form of

$$U(y)=U_0(y)+pU_1(y)+p^2U_2(y)+\cdots \tag{26}$$

$$\theta(y)=\theta_0(y)+p\theta_1(y)+p^2\theta_2(y)+\cdots \tag{27}$$

$$\varphi(y)=\varphi_0(y)+p\varphi_1(y)+p^2\varphi_2(y)+\cdots \tag{28}$$

where $v_i(y)$, $i=1,2,3,\ldots$ are functions yet to be determined. According to Eqs. (23)–(25) the initial approximation to satisfy boundary condition is [26]

$$U_0(y)=(1-y^2)Pr\,Re, \tag{29}$$

$$\theta_0(y)=0, \tag{30}$$

$$\varphi_0(y)=0, \tag{31}$$

Substituting Eqs. (26)–(28) into Eqs. (23)–(25) yields

$$Gr\times\theta_0(y)\times Pr-\varphi_0(y)\times N_r+\frac{\partial^2U_1(y)}{\partial y^2}=0, \tag{32}$$

$$N_b\times\frac{\partial\varphi_0}{\partial y}\times\frac{\partial\theta_0}{\partial y}+\left(\frac{\partial\theta_0}{\partial y}\right)^2N_t+\frac{\partial^2\theta_1}{\partial y^2}-U_0(y)+N_b+N_t=0, \tag{33}$$

$$\frac{\partial^2\varphi_1}{\partial y^2}+\frac{\left(\frac{\partial^2\theta_0}{\partial y^2}\right)\times N_t}{N_b}-10U_0(y)=0. \tag{34}$$

The solutions of Eqs. (32)–(34) may be written as follows:

$$U_1(y)=0, \tag{35}$$

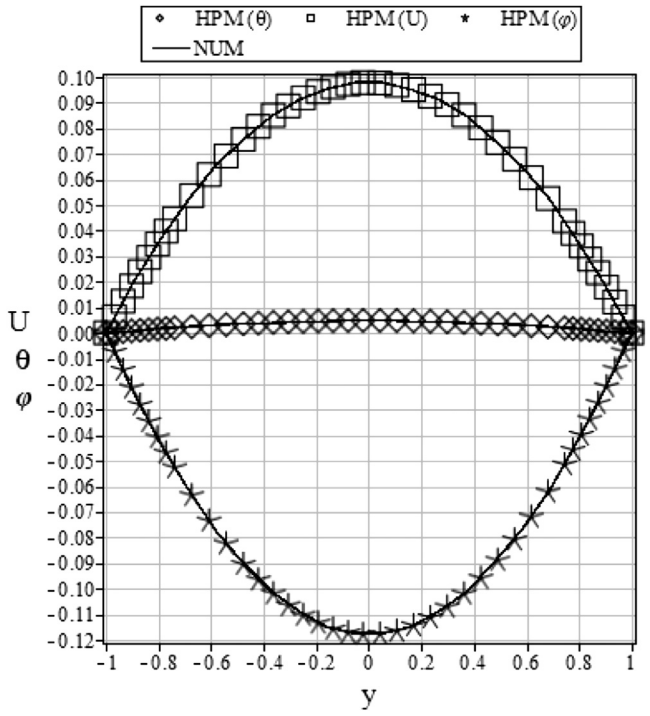

Fig. 2. Comparison of U, θ and ϕ versus the exact solution with the result obtained by HPM at N_t=N_b=N_r=0.1, Gr=0, Pr=1, σ=0, L_e=10.

$$\theta_1(y) = -Re\,Pr \times (0.083y^4 - 0.5y^2) + (0.5(-N_b - N_t))y^2 - 0.416Re\,Pr + 0.5N_b + 0.5N_t, \tag{36}$$

$$\varphi_1(y) = -0.83Re\,Pr \times y^4 + 5.Re\,Pr \times y^2 - 4.17Re\,Pr. \tag{37}$$

In the same manner, the rest of components were obtained by using the Maple package. According to the HPM, we can conclude ($Gr=\sigma=0$, $N_r=N_b=N_t=0.1$, $L_e=10$ and $Re=Pr=1$)

$$U(y) = 0.0049 + 3.34 \times 10^{-11}y^{12} + 0.001y^4 - 0.0000147y^6 - 3.02 \times 10^{-9}y^{10} - 0.0059y^2 + 5.498 \times 10^{-7}y^8 \tag{38}$$

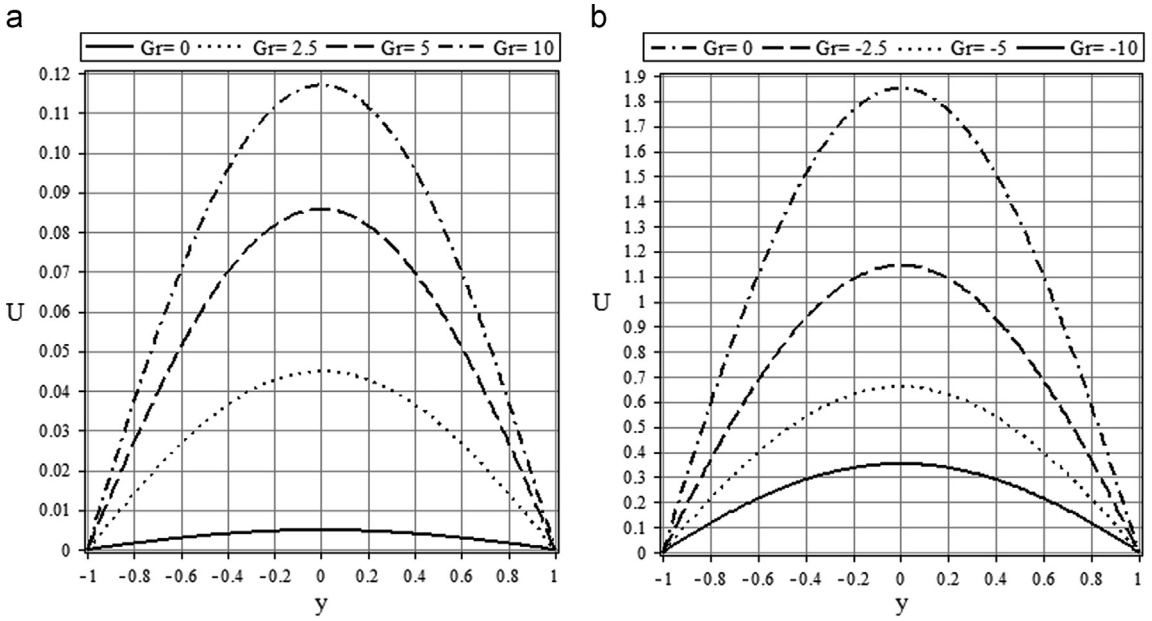

Fig. 3. (a) The dimensionless velocity profiles for various values of $Gr>0$ with $N_t=N_b=N_r=0.1$, $Pr=1$, $\sigma=0$, $L_e=10$. (b) The dimensionless velocity profiles for various values of $Gr<0$ with $N_t=N_b=N_r=0.1$, $Pr=1$, $\sigma=0$, $L_e=10$.

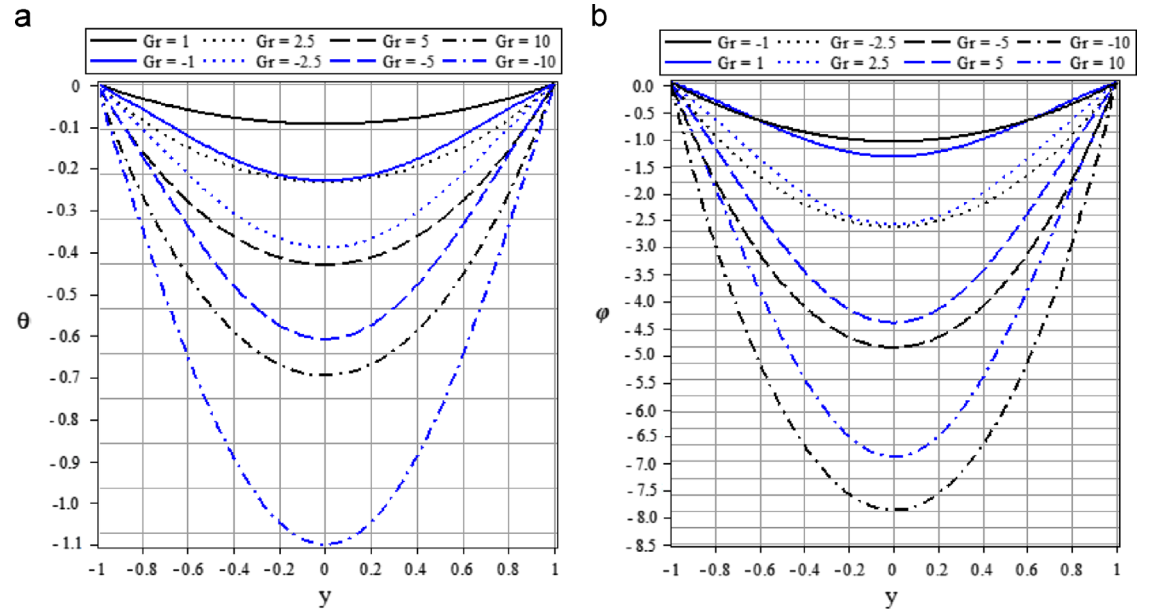

Fig. 4. (a) The dimensionless temperature profiles for various values of Gr with $N_t=N_b=N_r=0.1$, $Re=Pr=1$, $\sigma=0$, $L_e=10$. (b) The dimensionless nanoparticle volume fraction profiles for various values of Gr with $N_t=N_b=N_r=0.1$, $Re=Pr=1$, $\sigma=0$, $L_e=10$.

$$\theta(y) = 8.1 \times 10^{-11} y^{12} + 0.098 - 0.0004y^4 + 0.000022y^6 + 6.78 \times 10^{(-9)} y^{10} - 0.098y^2 + 3.948 \times 10^{-7} y^8 + 2.29 \times 10^{-13} y^{14} \quad (39)$$

$$\varphi(y) = -1.92 \times 10^{(-10)} y^{12} - 0.118 - 0.0046y^4 + 0.0003177438823y^6 + 5.648 \times 10^{-8} y^{10} + 0.12y^2 - 0.000003y^8 + 2.3 \times 10^{-12} y^{14} \quad (40)$$

and so on. In the same manner the rest of the components of the iteration formula can be obtained.

4. Results and discussion

To get better understanding of flow and heat transfer characteristics in the nanofluid, we thereafter make a detailed analysis on the problem of the fully developed nanofluid flow and heat transfer in a vertical channel. Comparison between the results of HPM and Numerical solution is shown in (Fig. 2). It can be seen that the HPM method is very close to Numerical solution, also Table 1 exhibit the numerical magnitude of U, θ and φ. The velocity profiles $U(Y)$ for various values

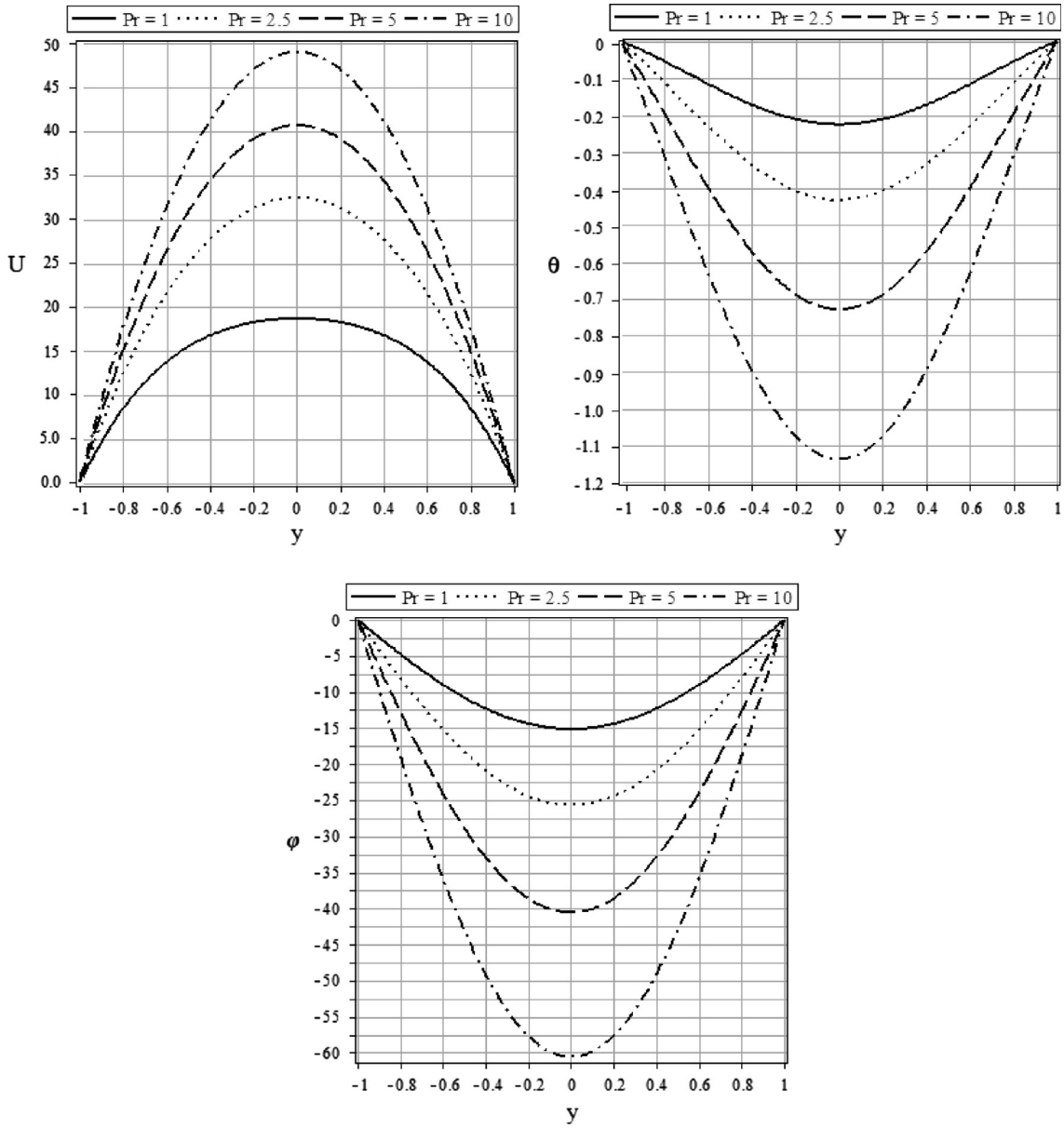

Fig. 5. The velocity, temperature and nanoparticle volume fraction profiles for various values of Pr in the case of $Gr=5$ with $N_t=N_b=N_r=0.2$, $\sigma=0$, $Re=1$, $L_e=10$.

of Gr in the case of $N_r=N_t=N_b=0.1$, $L_e=10$, $Re=Pr=1$ and $\sigma=0$ are presented in Fig. 3. It can be seen from Fig. 3a that for buoyancy-assisted case ($Gr>0$), the dimensionless velocities near the centerline of the channel decrease monotonously with the increase of Gr while the velocities in the vicinity of the walls increase continuously with the magnitude of Gr. Physically, this is due to the fact that, near the walls, the viscous force in the boundary layer plays an important role to keep the fluid attached and the increasing of buoyancy force immediately results in the enhancement of the velocity profiles. Simultaneously, due to the constraint of the mass flux conservation, the velocity profiles in the vicinity of the channel have to decrease. For the buoyancy-opposing case ($Gr<0$), as shown in Fig. 3b, the changing trend for velocities is quite similar to the buoyancy-assisted case, this is to say, the velocities near the centerline of the channels decrease as Gr enlarges. And the velocities in the vicinity of the walls increase as Gr evolves. The physical explanation is that in the buoyancy-opposing case, the buoyancy force plays a negative effect on the fluid motion in the boundary layer, which encumbers the increase of the velocity near the wall, while the velocity profiles near the channel center have to increase with the requirement of the mass flux conservation. The temperature distribution $\theta(Y)$ and nanoparticle volume fraction profiles for various values of Gr with

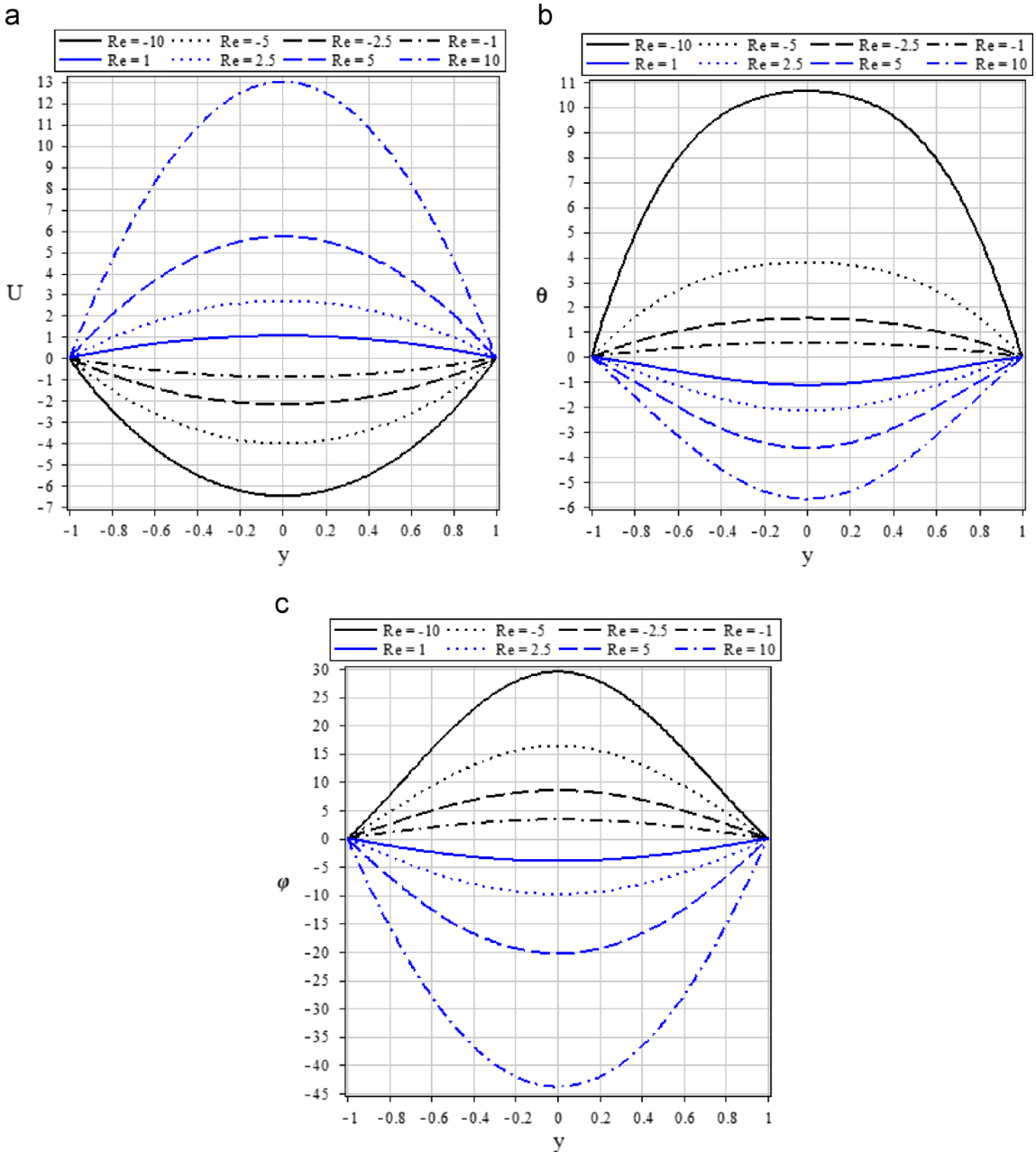

Fig. 6. The velocity, temperature and nanoparticle volume fraction profiles for various values of Re in the case of $Gr=5$ with $N_t=N_b=N_r=0.1$, $\sigma=0$, $Pr=1$, $L_e=10$.

$N_r=N_t=N_b=0.1$, $L_e=10$, $Re=Pr=1$ and $\sigma=0$ is plotted in Fig. 4. As shown in Fig. 4a, for the buoyancy-assisted case, the absolute amplitude for temperature profiles increases gradually with reduction of Gr owing to the effect of the fluid convection. Similar trend can be found for the buoyancy-opposing flow case, and the absolute amplitude for temperature profiles increases consecutively with increase of Gr. The nanoparticle volume fraction profiles show inverse changing trend as compared with the temperature profiles. As shown in Fig. 4b, with the same physical parameters, the absolute amplitude for $\varphi(Y)$ reduces with increasing of Gr for both the buoyancy-assisting and the buoyancy-opposing cases, but Gr exhibits more obvious effect on $\varphi(Y)$ than $\theta(Y)$. The effects of Prandtl number Pr on the flow are shown in Fig. 5. As illustrated in these figures, Pr plays important role on the three profiles. From Fig. 6, it is found that the velocity profiles $U(Y)$ increase rapidly as Pr evolves from 1 to 10. The temperature profiles $\theta(Y)$ vary in a quite different manner. Near the walls, the absolute amplitude for temperature deceases as Pr increases, while in the vicinity of the channel center, this amplitude enlarges gradually with increasing of Pr, as shown in Fig. 5. The changing trend for the nanoparticle volume profiles $\varphi(Y)$ is similar to the temperature change in the vicinity of the channel center. This is to say that the increasing of Pr immediately results in the enlargement of the absolute amplitude for $\varphi(Y)$. But the effect is more evident as compared with the temperature distribution, as shown in Fig. 5. The velocity, temperature and nanoparticle volume fraction profiles for various values of Re in the case of $Gr=5$ with $N_t=N_b=N_r=0.1$, $\sigma=0$, $Pr=1$, $L_e=10$ as shown in Fig. 6.

5. Conclusion

The laminar mixed convection flow of a nanofluid caused by both the external pressure gradient and the buoyancy force in a vertical channel has been investigated in detail. The four field equations which embody the conservation of total mass, momentum, thermal energy, and nanoparticle volume fraction have been reduced to three ordinary differential equations by means of a set of similarity variables. The accurate solutions have been given for both the buoyancy-assisted and the buoyancy-opposing cases. Using similarity variables, the governing partial differential equations are transformed to ordinary differential equations, which are solved along with the corresponding boundary conditions and the mass flux conservation relation by the homotopy perturbation method (HPM). The changing trends for the velocity profiles, the temperature profiles, and the nanoparticle volume fraction profiles against the Grashof number Gr have been illustrated, respectively. Besides, the effect of the Prandtl number Pr on the nanofluid flow has been discussed. It is found that Pr plays important roles on the three profiles, which develop dramatically as Pr evolves from1 to 10.

References

[1] Gebhart B, Jaluria Y, Mahajan RL, Sammakia B., Buoyancy-induced flows and transport hemisphere, New York; 1988.
[2] Martynenko OG, Khramtsov PP. Free-convective heat transfer. Berlin: Springer; 2005.
[3] Choi US. Enhancing thermal conductivity of fluids with nanoparticles. ASME FED 1995;231:99–103.
[4] Yu M, Lin J. Nanoparticle-laden flows via moment method: a review. Int J Multiphase Flow 2010;36:144–51.
[5] Das SK, Choi US, Yu W. Nanofluids sciences and technology. New Jersey: Wiley; 2008.
[6] Buongiorno J. Convective transport in nanofluids. ASME J Heat Transfer 2006;128:240–50.
[7] Daungthongsuk W, Wongwises S. A critical review of convective heat transfer nanofluids. Renewable Sustainable Energy Rev 2007;11:797–817.
[8] Ding Y, Chen H, Wang L, Yang CY, Hel Y, Yang W, et al. Heat transfer intensification using nanofluids. Kona 2007;25:23–38.
[9] Wang XQ, Mujumdar AS. A review on nanofluids—Part I: Theoretical and numerical investigations. Braz J Chem Eng 2008;25:613–30.
[10] Wang XQ, Mujumdar AS. A review on nanofluids—Part II: Theoretical and numerical investigations. Braz J Chem Eng 2008;25:631–48.
[11] Kaka S, Pramuanjaroenkij A. Review of convective heat transfer enhancement with nanofluids. Int J Heat Mass Transfer 2009;52:3187–96.
[12] Eastman JA, Choi SUS, Li S, Yu W, Thompson LJ. Anomalously increased effective thermal conductivities of ethylene glycol-based nanofluids containing copper nanoparticles. Appl Phys Lett 2001;78:718–20.
[13] Xie HQ, Lee H, Youn W, Choi M. Nanofluids containing multi walled carbon nanotubes and their enhanced thermal conductivities. J Appl Phys 2003;94:4967–71.
[14] Oztop HF, Abu-Nada E. Numerical study of natural convection in partially heated rectangular enclosures filled with nanofluids. Int J Heat Fluid Flow 2008;29:1326–36.
[15] Xuan YM, Li Q. Heat transfer enhancement of nanofluid. Int J Heat Fluid Flow 2000;21:58–64.
[16] Cimpean DS, Pop I. Fully developed mixed convection flow of a nanofluid through an inclined channel filled with a porous medium. Int J Heat Mass Transfer 2012;55:907–14.
[17] Lin J, Lin P, Chen H. Research on the transport and deposition of nanoparticles in a rotating curved pipe. Phys Fluids 2009;21:122001.
[18] Lin PF, Lin JZ. Prediction of nanoparticle transport and deposition in bends. Appl Math Mech 2009;30(8):957–68, http://dx.doi.org/10.1007/s10483-009-0802-z.
[19] Lavine AS. Analysis of fully developed opposingmixed convection between inclined parallel plates. Wärme-und Stoffubertragung 1988;23:249–57.
[20] Chen YC, Chung JN. The linear stability of mixed convection in a vertical channel flow. J Fluid Mech 1996;325:29–51.
[21] Kuznetsov AV, Nield DA. Natural convective boundary-layer flow of a nanofluid past a vertical plate. Int J Therm Sci 2010;49(2):243–7.
[22] Ajadi SO, Zuilino M. Approximate analytical solutions of reaction–diffusion equations with exponential source term: homotopy perturbation method (HPM). Appl Math Lett 2011;24(10):1634–9.
[23] Slota D. The application of the homotopy perturbation method to one-phase inverse Stefan problem. Int Commun Heat Mass Transfer 2010;37(6):587–92.
[24] Fakour M, Ganji DD, Vahabzadeh A, Kachapi SHH. Accuracy of VIM, HPM and ADM in solving nonlinear equations for the steady three-dimensional flow of a Walter's B fluid in vertical channel. Walailak J Sci Technol 2014;11(7):593–609.
[25] Hosein Nia SH, Ranjbar AN, Ganji DD, Soltani H, Ghasemi J. Phys Lett A 2008;372(16):2855–61.
[26] Xu H, Fan T, Pop I. Analysis of mixed convection flow of a nanofluid in a vertical channel with the Buongiorno mathematical model. Int Commun Heat Mass Transfer 2013;44:15–22.